\$ SUPER

Contents lists available at ScienceDirect

Microchemical Journal

journal homepage: www.elsevier.com/locate/microc





Circular DNA enhanced amplification-free CRISPR/Cas12a assays for end-user friendly ultra-sensitive *Porphyromonas gingivalis* diagnosis

Xuan Wu^{a,h,i}, Ning-Ning Pi^a, Fei Deng^{d,e}, Shi-Yang Tang^{f,g}, Cheng-Chen Zhang^f, Lu Zhu^a, Fang-Fang Sun^a, Xiao-Yao He^a, Han-Qing Li^a, Shi-Long Zhaoⁱ, Rong Xiang^{c,*}, Yi Li^{b,d,e,*}

- ^a Key Laboratory of Environmental Chemistry and Ecotoxicology of Organic Pollutants of Chongqing, Ecological and Environment Monitoring Center of Chongqing, 252 Qishan Road, Chongqing 401132, China
- b Key Laboratory of Clinical Laboratory Diagnostics (Ministry of Education), College of Laboratory Medicine, Chongqing Medical University, Chongqing 400016, China
- c Precision Medicine Center, The Second Affiliated Hospital of Chongqing Medical University, 288 Tianwen Road, Chongqing 400010, China
- d Western(Chongqing) Collaborative Innovation Center for Intelligent Diagnostics and Digital Medicine, Chongqing National Biomedicine Industry Park, No. 28 Gaoxin Avenue, High-tech Zone, Chongqing 401329, China
- ^e ARC Centre of Excellence for Nanoscale Biophotonics, Graduate School of Biomedical Engineering, Faculty of Engineering, University of New South Wales, Sydney 2052, Australia
- ^f School of Electronics and Computer Science, University of Southampton, Southampton SO17 1BJ, UK
- g School of Mechanical and Manufacturing Engineering, University of New South Wales, Sydney, NSW 2052, Australia
- h Hospital/School of Stomatology, Zunyi Medical University, 143 Dalian Road, Guizhou 563006, China
- ⁱ Hunan Provincial Key Laboratory of Medical Virology, College of Biology, Hunan University, 27 Tianma Road, Hunan 410082, China

ARTICLE INFO

Keywords: Porphyromonas gingivalis Ultra-sensitive CRISPR biosensor Amplification-free Point-of-Care diagnosis End-user friendly

ABSTRACT

Periodontitis not only leads to tooth loss but is also associated with various systemic symptoms. Porphyromonas gingivalis (Pg) is the microorganism most closely linked to periodontitis. A rapid and accurate Pg detection method holds significant potential health benefits for patients. While several nucleic acid amplification-based diagnostic methods have been developed, there is a current lack of rapid diagnostic tools for Pg, particularly at chair-side level. Here, two detection methods for the Pg 16S gene based on the CRISPR/Cas12a system have been developed. To achieve ultra-high sensitivity in the developed CRISPR/Cas12a assays without preamplification, we designed a circular DNA molecule (termed as Cir-amplifier) which amplifies the signal output of the Cas12a reactions in a cascade response manner. The Cir-amplifier enhanced Fluorescence-Cas12a reaction achieved a minimum detectable limit of 0.39 CFU of Pg within 80-minute under room-temperature. In addition, the Cir-amplifier enhanced Lateral Flow Detection (LFD)-Cas12a reaction has demonstrated the ability to detect a minimum of 3.9 CFU of Pg in 90 min, with results observable by the naked eye. The potential of the two methods for Pg detection in clinical samples has been demonstrated, showing 100 % sensitivity compared to the traditional real-time PCR method. In summary, we have established two efficient detection methods for Pg that eliminate the need for pre-amplification, hence no amplicon contaminations, making them promising candidates for chair-side Pg diagnosis. Furthermore, the Cir-amplifier has been demonstrated to be adaptable to CRISPR/Cas systems producing various signal formats. The Cir-amplifier is expected to become a universal CRISPR/Cas enhancer.

1. Introduction

Periodontitis, characterized by bacteria-induced inflammation of the periodontal tissues, stands as the sixth most prevalent chronic inflammatory ailment globally [1]. According to NHANES (National Health and Nutrition Examination Survey) data, severe periodontitis affects

over 700 million people [2]. And periodontitis leads to the gradual loss of supporting alveolar bone around teeth, potentially resulting in tooth mobility and loss [3]. Research conducted on both animals and humans has established correlations between periodontitis and various conditions, including diabetes [4], cardiovascular diseases [5], Alzheimer's disease [6], and adverse pregnancy outcomes [7]. Among the bacteria

E-mail addresses: xiangrong@hospital.cqmu.edu.cn (R. Xiang), yi.li@cqmu.edu.cn (Y. Li).

^{*} Corresponding authors at: Key Laboratory of Clinical Laboratory Diagnostics (Ministry of Education), College of Laboratory Medicine, Chongqing Medical University, Chongqing 400016, China (Y. Li).

associated with periodontitis, *Porphyromonas gingivalis* (*Pg*) is particularly noteworthy as a highly pathogenic species and a significant biomarker [8–10]. Early detection of these periodontal pathogens holds immense potential for improving patients' overall health.

Polymerase chain reaction (PCR), as a representative of nucleic acid detection methodologies, offer remarkably enhanced sensitivity of Pg detection in comparison to traditional cultivation techniques [11,12]. However, these techniques necessitate relatively sophisticated laboratory equipment, such as a dedicated thermocycler or in combination of subsequent electrophoresis and gel imaging systems, etc., thereby limiting their potential for chair-side Pg detection at end-user friendly settings.

To address this limitation, efforts have been focused on simplifying the required equipment and enabling visually interpretable results by integrating PCR or isothermal amplification with microfluidic chip technologies [8,13]. Despite the remarkable specificity and sensitivity PCR-based methods achieved in identifying target sequences, it's important to recognize that sequence amplification-based methods inherently produce an excess of target sequences, or called amplicons. These amplicons can easily disperse into the environment, potentially forming aerosols, which raises concerns about aerosol pollution during the detection process. Such pollution could subsequently lead to false positive outcomes [14].

Emerging as an innovative and essential toolbox for genome editing, CRISPR/Cas biotechnology possesses unparalleled precision in identifying and cleaving distinct DNA and RNA sequences. Certain Cas orthologues, such as Cas13 [15] and Cas12a [16], also exhibit unique non-specific collateral enzymatic activities (trans) following targetspecific sequence recognition. This trans activity can be leveraged to release fluorescent signal from designated fluorescent-quenched probes efficiently, leading to the generation of a distinctive fluorescent signal. This strategy demonstrates a remarkable combination of high specificity and sensitivity for nucleic acid detection assays. Furthermore, it offers facile adaptability, requiring only the substitution of the guide RNA (gRNA) of Cas ribonucleoprotein (RNP) to detect diverse targets. Based on this principle, the CRISPR/Cas system has found widespread applications in nucleic acid detection. For example, early-stage platforms such as DETECTR and SHERLOCK utilize isothermal amplification techniques in combination with CRISPR/Cas12a, Cas13a, and Cas14 to achieve highly sensitive detection of target sequences at the attomole level, while also enabling the discrimination of genotypes and single nucleotide polymorphisms (SNPs) within target sequences [17–19]. In recent years, CRISPR/Cas-based biosensing approaches have been extensively employed in the development of high-sensitivity detection methods targeting various pathogens, including Zika virus (ZIKV) [20], SARS-CoV-2 [21], and Listeria monocytogenes [22] etc. However, achieving high sensitivity in the aforementioned CRISPR/Cas detection methods requires pre-amplification of the target sequences. This step not only extends the detection timeline but also introduces a substantial number of unintended target sequences, similar to PCR approaches, thereby posing a risk of aerosol contamination.

We previously discovered that a specifically designed circular DNA nanostructure can be applied to induce an autocatalysis reaction for CRISPR/Cas *trans*-cleavage, hence, eliminating the need for additional nucleic acid amplification to reach aM level (\sim 1 copy/ μ L) sensitivity [23]. This unique circular DNA nanostructure, named Cir-amplifiers, consists of an 18 bp double-stranded region and a 3 nt single-stranded linker. In this study, we further demonstrated the potential of the Ciramplifiers in dealing with broader pathogenic detection, here Pg. More importantly, optimal reaction condition has been investigated to reduce overall background signals, and the autocatalysis reaction targeting Pg has been transferred to a Fluorescence- and Lateral Flow Detection (LFD)-Cas12a assays, resulting in two user-friendly, pre-amplification-free Point-of-Care (POC) Pg DNA detection methods, with limits of detection (LoD) of 0.39 and 3.9 colony-forming unit (CFU) respectively.

2. Materials and methods

2.1. Bacterial strains and culture conditions

The strain *Pg* W83 was employed for the development of detection methods. Additionally, eight other bacterial strains were utilized to assess the specificity of both assays. All the strains used in this study were purchased from American Type Culture Collection (ATCC) (Table S1). W83 was cultured in brain heart infusion (BHI) broth (Oxoid, Basingstoke, United Kingdom) supplemented with 5 mg/L hemin (Aladdin Scientific, Shanghai, China) and 5 mg/L menadione (Aladdin Scientific, Shanghai, China) under anaerobic conditions at 37°C, with shaking at 150 RPM for 2 to 3 days. The remaining bacterial strains listed in Table S1 were cultured following the recommended protocols by the ATCC.

2.2. Measurement of bacterial Suspension concentration

To determine the CFU number of W83, serial dilutions of bacteria were prepared at ten-fold concentrations using 0.01 M phosphate-buffered saline (PBS) (Aladdin Scientific, Shanghai, China), and then, $100~\mu L$ aliquots of each dilution were plated on Gifu Anaerobic Medium agar plates (Solarbio, Beijing, China) supplemented with 1 mg/L menadione and 5 % defibrinated sheep blood (Thermo Fisher Scientific, Shanghai, China). The plates were incubated at 37 $^{\circ} C$ under anaerobic conditions for a period ranging from 5 to 8 days; subsequently, CFU counts for strain W83 were recorded.

2.3. Design of oligo RNA and DNA

All oligo RNA and DNA were synthesized by Tsingke Biotech (Beijing, China). The detailed sequences and modified moieties are presented in Table S2. Primers for RT-PCR assays were designed based on homologous sequences within the *Pg* 16S rRNA gene using Primer Premier 6 software (PREMIER Biosoft, Palo Alto, USA), with default primer parameters. The RT-PCR serves as a reference method for the detection of clinical samples. In the Cas12a assays, the sequence of gRNA was determined based on the protospacer adjacent motif (PAM) found in homologous sequences within the *Pg* 16S rRNA gene. According to previous reports, hairpin structures in reporter have been found to enhance Cas *trans*-cleavage activity [24,25]. In this study, two types of reporters were employed to compare their effectiveness: one consisting of a linear reporter composed of a 5-nt poly-T sequence, and the other featuring a hairpin structure within the reporter.

In our previous study, variations in the length of the double-stranded region of the Cir-amplifier resulted in varying degrees of background signal [23]. To maximumly minimize background signal, we designed three distinct Cir-amplifier variants with varying lengths of doublestranded regions, specifically 14 bp (Linear ssDNA 3), 18 bp (Linear ssDNA 2), and 22 bp (Linear ssDNA 1), all of which included a linker (TT) and PAM region (TTTC) (Table S2). To obtain these Cir-amplifier variants, three different lengths of ssDNA were synthesized, and modifications were introduced at their 5' and 3' ends as well as at the sixth T base (Fig. 2A). Specifically, biotin, CHCH, and Azide (N3) modifications were incorporated. The CHCH and Azide (N3) modifications were utilized to facilitate the circularization of ssDNA. Biotin was employed to enable the binding of ssDNA to streptavidin-modified magnetic beads (1 μm, MCE, Shanghai, China), enhancing the single-molecule circularization efficiency. Simultaneously, corresponding cDNA sequences were also synthesized. Detailed steps for Cir-amplifier synthesis are outlined in the subsequent section 2.5.

2.4. Standard Fluorescence-Cas12a assay

We first established a standard Fluorescence-Cas12a reaction to verify the designed RNP's ability to recognize the *Pg* 16S gene and cleave

FRET-ssDNA reporters, thereby generating a fluorescence signal. This was used to compare the signal intensities produced by linear and hairpin reporters.

In Fluorescence-Cas12a reactions, a FRET-ssDNA reporter modified with Texas Red at the 5' end and BHQ-2 at the 3' end was utilized. When the RNP recognized the target 16S sequence, its *trans* activity was activated, initiating the cleavage of FRET-ssDNA reporters and resulting in the separation of the Texas Red fluorophore and BHQ-2 quencher, which released a fluorescence signal (Fig. 1A).

The Fluorescence-Cas12a reaction mixture included: 10 μ L of 10 \times NEB 2.1 buffer, 6 pmol of Cas12a protein (NEB, Beijing, China), 6 pmol of gRNA, 20 pmol of FRET-ssDNA reporter, 1 μ mol DTT, and a final volume of ddH₂O up to 100 μ L with Pg DNA as the target. After thorough mixing, the reaction mixture was incubated for 60 min at room temperature. Fluorescence measurements were acquired every 15 min using the EnSight Multimode Plate Reader (PerkinElmer, Massachusetts, USA) at an excitation wavelength of 570 nm and an emission wavelength of 615 nm.

2.5. Synthesis and characterization of Cir-amplifier

In classical Cas detection methods, pre-amplification is typically required to increase the copy number of target sequences in the reaction mixture, ensuring sufficient activation of RNPs for satisfactory sensitivity. To achieve high sensitivity in target sequence detection using the Cas12a reaction without pre-amplification, we designed a circular DNA structure called Cir-amplifier, which contains a segment of the target sequence but cannot activate the RNPs in its circular form. This structure

includes a short single-stranded segment that can be cleaved by the *trans*-activity of RNPs, leading to re-linearization. The re-linearized Ciramplifier can then activate more RNPs, creating a cascade reaction. To this end, we synthesized and characterized three differently sized Ciramplifiers.

First, we accomplished the circularization of modified linear ssDNA (Table S2) by employing a click chemistry method as previously described [23]. In brief, 400 µL of 2 mg/mL streptavidin-modified magnetic beads (1 µm) (MCE, Shanghai, China) were initially blocked for 1 h using a 1 % (w/v) BSA solution to eliminate non-specific binding. Then, these beads were incubated with 1 mL of the modified linear ssDNA oligo at a concentration of 0.5 μM for an additional hour to facilitate biotin-streptavidin binding. Afterwards, the beads were washed with PBS to eliminate any residual free linear ssDNA oligo. Subsequently, 1 mL of a click chemistry reaction solution containing 1 mM CuSO₄, 2 mM Tris(2-carboxyethyl)phosphine (TCEP), and 100 μM Tris[(1-benzyl-1H-1,2,3-triazol-4-yl)methyl]amine (TBTA) was added to the beads and incubated for 12 h at room temperature to facilitate synthesis. After incubation, the beads were collected and washed with PBS again before adding 10 units of Exonuclease VII (NEB, Beijing, China) and incubating at 37°C for 30 min to remove any remaining linear ssDNA fractions. Following another wash, the circularized ssDNA was released from the streptavidin-modified beads by heating at 95°C for 30 min; subsequently, the supernatant containing the released circularized ssDNA was collected, and the synthesis of the circularized ssDNA was identified through 10 % agarose gel electrophoresis (w/v) and visualized with the Bio-Rad Gel Doc XR + imaging system (Bio-Rad Laboratories Inc., Hercules, USA). The concentration of circularized

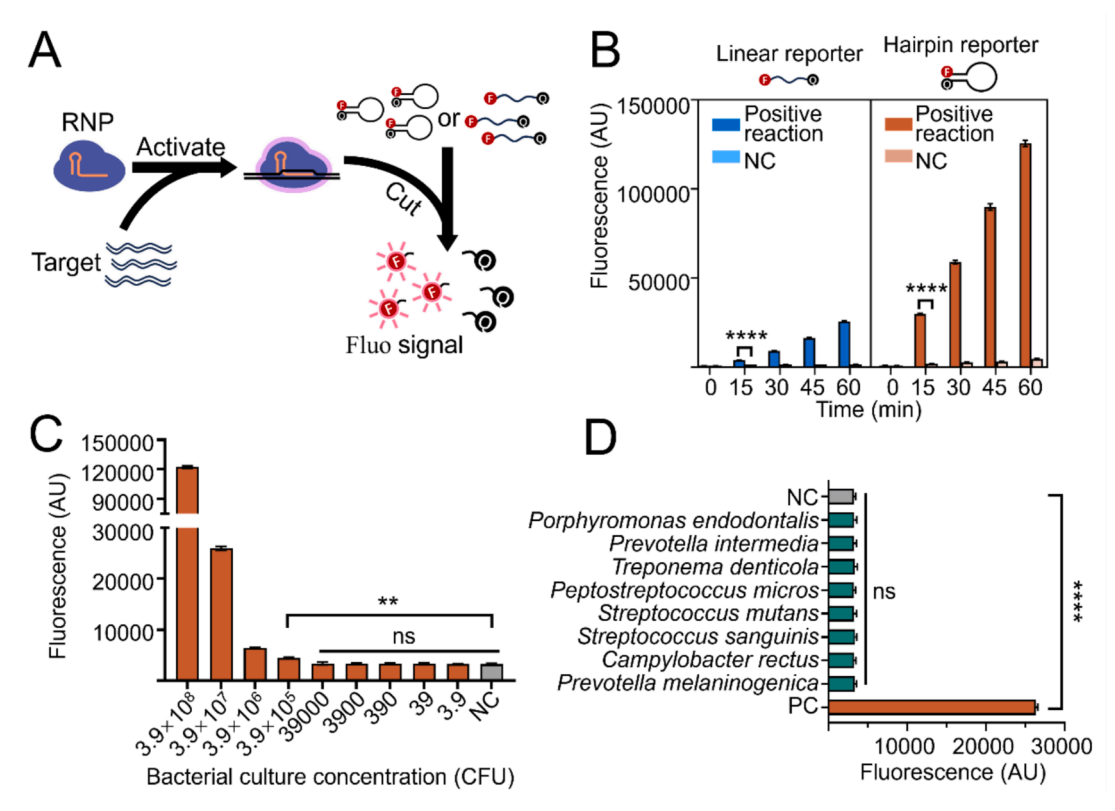


Fig. 1. Fluorescence-Cas12a Assays for the Detection of Pg. (A) Schematic representation of the fluorescence-Cas12a assay. The red solid circle labeled "F" represents the Texas red fluorescence moiety, while "Q" denotes the BHQ-2 quencher moiety. (B) Comparison between the hairpin and linear reporters. Values represent mean \pm SEM (n = 3, two-tailed Student t-test; ****, p < 0.0001). (C) LoD for the fluorescence-Cas12a assay. The X-axis depicts the W83 bacterial load used for the fluorescence-Cas12a reaction, expressed in Colony Forming Units (CFU). The negative control (NC) does not include DNA trigger. Values represent mean \pm SEM (n = 3, two-tailed Student t-test: **, p < 0.01; one-way ANOVA: ns, not significant). (D) Specificity analysis of the fluorescence-Cas12a assay. The positive control (PC) involves target DNA from 3.9×10^7 CFU of Pg W83 strain. The NC does not include DNA trigger. Values represent mean \pm SEM (n = 3, two-tailed Student t-test: ****, p < 0.0001; one-way ANOVA: ns, not significant). (For interpretation of the references to color in this figure legend, the reader is referred to the web version of this article.)

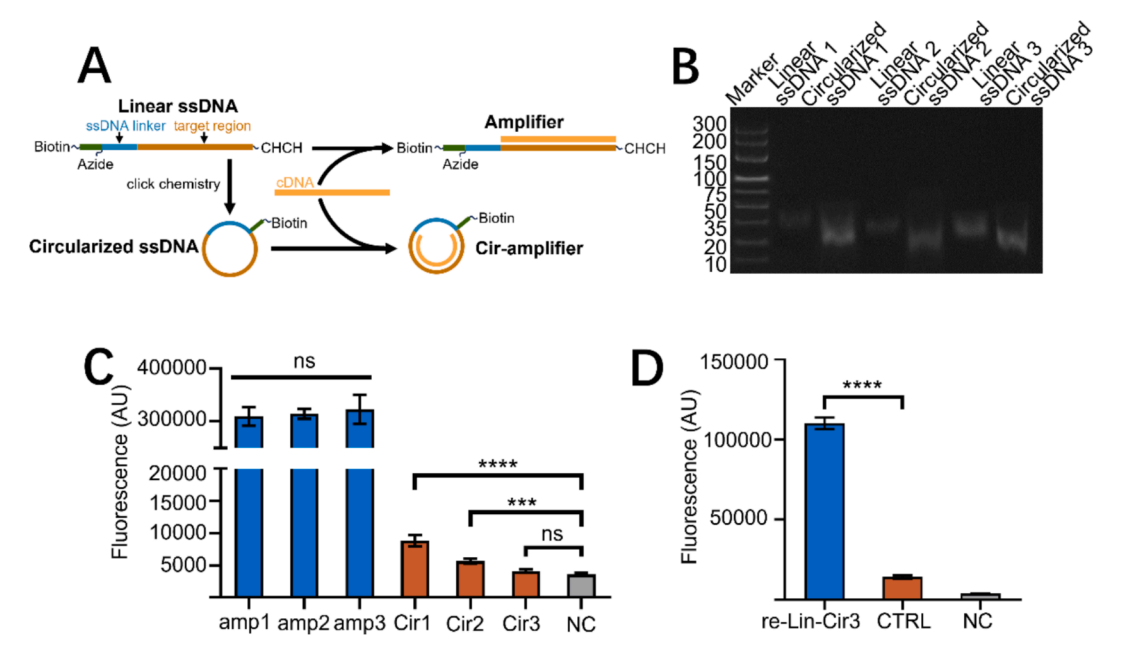


Fig. 2. The verification of the activation capability of the Cir-amplifier. (A) The preparation process of Cir-amplifier. (B) Gel electrophoresis of circularized ssDNA. (C) Background values caused by Cir-amplifier. amp, amplifier; Cir, Cir-amplifier; NC, negative control, a control reaction without the amplifier and Cir-amplifier. Values represent mean \pm SEM (n = 3, two-tailed Student *t*-test: ***, p < 0.001; ****, p < 0.0001; one-way ANOVA: ns, not significant). (D) Verification of re-linearized Cir-amplifier initiating Cas reaction. re-Lin-Cir, re-linearized Cir-amplifier; CTRL, a reaction containing an equal amount of activated RNP-0 as in the re-Lin-Cir reaction; NC, negative control, a control reaction without trigger DNA, re-Lin-Cir, and RNP-0. Values represent mean \pm SEM (n = 3, two-tailed Student *t*-test; ****, p < 0.0001).

ssDNA was determined using Nanodrop (Thermo Fisher Scientific, Waltham, USA). Then equimolar amounts of circularized ssDNA and corresponding cDNA were mixed together to form the Cir-amplifier (Fig. 2A). The incubation steps were conducted in a Bio-Rad PCR instrument model T100 (Bio-Rad Laboratories Inc., Hercules, USA).

The circular configuration of the Cir-amplifiers effectively blocks their activation of RNPs, a key hypothesis of this study. To test this hypothesis, the Cir-amplifiers were added to the Fluorescence-Cas12a reaction mixture to see if they would indeed activate the RNPs. The reaction mixture included 10 μL of 10 \times NEB 2.1 buffer, 6 pmol of Cas12a protein, 6 pmol of gRNA gRNA targeting Pg, 20 pmol of FRET-ssDNA reporter, 1 μmol of DTT, and a final volume of ddH₂O up to 100 μL with 25 nM Cir-amplifier. After incubating at room temperature for 60 min, the fluorescence intensity was measured at an excitation wavelength of 570 nm and an emission wavelength of 615 nm.

The recognition of the re-linearized Cir-amplifier by the RNP, along with the activation of the RNP's trans-activity, is crucial for initiating the subsequent cascade reaction. To further confirm this mechanism, we employed a pre-activated Cas12a designed elsewhere targeting the N gene of Langya henipavirus, termed RNP-0 (Cas12a + gRNA-0) to relinearize the Cir-amplifier (sequence of gRNA-0 is listed in Table S2). The reaction mixture comprised 10 μL of 10 \times NEB 2.1 buffer, 6 pmol of Cas12a protein, 6 pmol of gRNA-0, 25 nM Cir-amplifier, 1 μ mol of DTT, 1.1 pmol of RNP-0 activator (dsDNA fragment recognized by gRNA-0), and a final volume of ddH2O up to 100 µL. After a 1-hour reaction, $10~\mu L$ of the RNP-0 reaction product, containing the re-linearized Ciramplifier, was transferred to a Pg Cas12a reaction system lacking the trigger sequence. The reaction system included 10 μL of 10 \times NEB 2.1 buffer, 6 pmol of Cas12a protein, 6 pmol of gRNA targeting Pg, 20 pmol of FRET-ssDNA reporter, 1 µmol of DTT, and a final volume of ddH₂O up to 100 μ L, with 10 μ L of the RNP-0 cleavage product. Considering that the reaction product contains both re-linearized Cir-amplifier and the activated RNP-0 with inherent trans ssDNA endonuclease activity, to demonstrate that the fluorescence signal generated in the subsequent Pg Cas12a reaction is a result of re-linearized Cir-amplifier activating RNP, we established a control group (CTRL) containing an equivalent amount

of activated RNP-0, mirroring the 10 μL RNP-0 product. The control reaction system consisted of 10 μL of 10 \times NEB 2.1 buffer, 0.6 pmol of Cas12a protein, 0.6 pmol of gRNA-0, 20 pmol of FRET-ssDNA reporter, 1 μmol of DTT, 0.11 pmol of RNP-0 activator, and a final volume of ddH₂O up to 100 μL . After a 1-hour reaction at room temperature, the fluorescence was measured at an excitation wavelength of 570 nm and an emission wavelength of 615 nm.

2.6. Cir-amplifier enhanced Fluorescence-Cas12a assay for Pg detection

After characterizing the performance of the Cir-amplifier, we incorporated it into the Fluorescence-Cas12a assay to enhance sensitivity. Increasing the amount of Cir-amplifier (Cir) leads to stronger signal amplification, but also results in higher background levels. Consequently, we initially evaluated the background fluorescence caused by various concentrations of Cir-amplifier (25-400 nM) and the fluorescence generated by corresponding amounts of linear amplifiers (amp) activating RNPs. The reaction systems included 10 μL of 10 \times NEB 2.1 buffer, 6 pmol of Cas12a protein, 6 pmol of gRNA targeting Pg, 20 pmol of FRET-ssDNA reporter, 1 µmol of DTT, 25-400 nM of linear amplifiers or Cir-amplifiers, DNA of 3.9×10^4 CFU of W83, and a final volume of ddH₂O up to 100 µL. Fluorescence values were measured after a 1-hour incubation at room temperature. Subsequently, the sensitivity of the Ciramplifier enhanced Fluorescence-Cas12a assay was determined using a 10-fold gradient dilution of Pg DNA. The reaction system comprised 10 μL of 10 \times NEB 2.1 buffer, 6 pmol of Cas12a protein, 6 pmol of gRNA targeting Pg, 20 pmol of FRET-ssDNA reporter, 1 µmol of DTT, 200 nM of Cir-amplifier, DNA ranging from 0.39 to 3.9×10^4 CFU of Pg W83. The reaction was conducted at room temperature for 120 min, with fluorescence values measured every 20 min.

2.7. LFD-Cas12a assays for Pg detection

To develop a more easily observable *Pg* detection method, we further integrated the Cas12a reaction with LFD. Biotin- and FITC-dual-labeled reporters in the Cas12a reaction act as bridges to fix gold nanoparticles

(AuNPs) on line 1 (test line) of the LFD, displaying red. When the target is present, some reporters are cleaved, reducing the AuNPs on line 1 (test line) and fading the red color. Since the outcome relies on the color intensity of line 1 (test line), and the reporter amount directly affects this intensity, we first optimized the quantity of the reporter. The reaction mixture included 10 μL of 10 \times NEB 2.1 buffer, 6 pmol of Cas12a protein, 6 pmol of gRNA targeting Pg, various amounts of reporter (0.2, 2, 20 pmol), 1 μmol of DTT, and ddH₂O to reach a final volume of 100 μL, with target DNA. After 15, 30, and 60 min of Cas12a reaction, a 20 µL aliquot of the reaction product was mixed with 80 μL of HybriDetect Assay Buffer (Milenia Biotec, Gießen, Germany). Subsequently, 50 µL of this mixture was incrementally dispensed onto the sample pad of the LFD (Milenia Biotec, Gießen, Germany) which has streptavidin immobilized at line 1 (test line) and a secondary antibody at line 2 (control line) (Fig. 4A). After 15 min, the results were observed visually, and the grayscale of line 1 (test line) was measured using ImageJ software [26]. The normalized grayscale (G) was calculated using the provided equation:

$$G = \frac{grayscale\left(sample\right)}{grayscale\left(NC\right)} \times 100\%$$

Later, the sensitivity of the LFD-Cas12a assay was determined. The reaction system included 10 μ L of 10 \times NEB 2.1 buffer, 6 pmol of Cas12a protein, 6 pmol of gRNA targeting Pg, various amounts of reporter (0.2, 2 pmol), 1 μ mol of DTT, and ddH₂O added to reach a final volume of 100 μ L, with tenfold serially diluted Pg DNA.

Similar to the Fluorescence-Cas12a assay, the Cir-amplifier was introduced into LFD-Cas12a to enhance the detection sensitivity. Considering that both the reporter and the Cir-amplifier are modified with biotin and may competitively bind to streptavidin on line 1 (test line), we optimized the ratio of reporter and Cir-amplifier. The reaction system comprised 10 μL of 10 \times NEB 2.1 buffer, 6 pmol of Cas12a protein, 6 pmol of gRNA targeting Pg, various amounts of reporter (0.2, 2, 20 pmol), 1 μ mol of DTT, 0–400 nM Cir-amplifier, and ddH₂O added to reach a final volume of 100 μL . After a 1-hour Cas12a reaction, a 20 μL aliquot of the product was mixed with 80 μL of HybriDetect Assay Buffer (Milenia Biotec, Gießen, Germany). 50 μL of this mixture were then gradually applied to the sample pad of the LFD (Milenia Biotec, Gießen, Germany). The grayscale of line 1 (test line) was subsequently measured using ImageJ software (Rasband, ImageJ, NIH, USA), and the G value was calculated.

After determining the ratio of the reporter and Cir-amplifier, the sensitivity of the Cir-amplifier enhanced LFD-Cas12a reaction was tested using a 10-fold gradient of Pg DNA. The reaction mixture consisted of 10 \times NEB 2.1 buffer, 6 pmol of Cas12a protein, 6 pmol of gRNA targeting Pg, 2 pmol reporter, 1 µmol of DTT, 200 nM Cir-amplifier, and sufficient ddH₂O to achieve a final volume of 100 µL. After incubating for 30, 60, 90, or 180 min, the products were transferred to an LFD and the G value was calculated as above mentioned.

2.8. Clinical sample studies

To further assess the performance of the newly developed Cas12a assays in detecting Pg in clinical samples, we employed 131 plaque samples to examine the concordance of the detection results between these new Cas12a assays and conventional RT-PCR assay. The plaque samples were collected as previously described elsewhere [11]. Briefly, supragingival plaque was meticulously removed from the sampling site. Sterile paper points were then inserted into periodontal pockets approximately 5 mm for 20 s, and subsequently stored at $-80~^{\circ}\text{C}$ until the detection of Pg DNA. An RT-PCR method, in which the primers target the same region as the gRNA, was built and served as the reference method for the evaluation of the accuracy of the Cas12a assays in clinical sample testing. The RT-PCR assays were performed with a final volume of 20 μ L containing 10 μ L of 2 \times SsoFastTM EvaGreen® Supermix (Bio-Rad, Hercules, USA), 10 pmol of each primer, and 1 μ L of

Pg DNA as template in ddH_2O . The parameters included an initial denaturation at 95°C for 30 s followed by amplification consisting of denaturation at 95°C for 5 s and annealing/extension for another 5 s at 56°C over a total of 39 cycles. Data analyses were carried out using Bio-Rad CFX Maestro 1.1 software (Bio-Rad, Hercules, USA).

2.9. Statistical analysis

Statistical significance in fluorescence and G values was analyzed using Student's t-test for differences between two groups and one-way ANOVA for multiple group comparisons with GraphPad Prism version 8 (GraphPad Software Inc., USA). Differences were considered significant at "P < 0.05, "*P < 0.01, "**P < 0.001, or ****P < 0.0001 in t-test, and tP < 0.05, tP < 0.01, or tP < 0.001 in ANOVA.

3. Results

3.1. Identification of Pg DNA by Fluorescence-Cas12a assay

To assess the capability of the designed Fluorescence-Cas12a assay recognizing the Pg 16S gene and generating a fluorescent signal, as well as to evaluate the efficiency of the linear and hairpin reporters in producing fluorescence signals (Fig. 1A), DNA extracted from 3.9×10^8 CFU of Pg was introduced into the Fluorescence-Cas12a reaction. After 15 min at room temperature, both linear and hairpin reporters exhibited significantly higher fluorescence values compared to the negative control (NC) without target DNA (Fig. 1B). This suggests that the RNPs effectively identify the target sequence and subsequently cleave the reporter.

In the comparison between the hairpin and linear reporters, the fluorescence signal produced by the hairpin reporter upon cleavage was significantly stronger than that produced by the linear reporter. Furthermore, the fluorescence signal generated by the hairpin reporter after a 15-minute reaction was significantly stronger than the signal produced by the linear reporter after a 60-minute reaction (Fig. 1B and S1). Regarding sensitivity, when using the hairpin reporter, the LoD for the 60-minute Fluorescence-Cas12a assay was 3.9×10^5 CFU of Pg, while for the linear reporter, it was 3.9×10^6 CFU Pg (Fig. 1C and S2), which is a 1 log difference caused by reporters. This indicates that owing to the higher cleavage efficiency of Cas12a on the hairpin reporter [24], the use of hairpin reporter not only reduces reaction time but also enhances sensitivity by tenfold. Hence, all subsequent Cas12a reactions utilized the hairpin reporter.

In terms of specificity, due to the specifically designed complementary binding of the gRNA to the *Pg* 16S gene, the Fluorescence-Cas12a assay in this study only responded to the *Pg* DNA and did not exhibit cross-reactivity with DNA from eight other common oral bacterial species (Fig. 1D).

3.2. Characterization of the Cir-amplifier

Previous reports indicate that the PCR detection method for *Pg* has a sensitivity of 100 CFU [11]. While the Fluorescence-Cas12a assay produced observable signals for *Pg* DNA, its sensitivity did not meet expectations. To improve the assay's sensitivity without introducing a preamplification step, we synthesized a series of Cir-amplifiers. The Ciramplifiers comprise a double-stranded target region capable of specifically activating the *trans* endonuclease activity of the RNP, and a polyT single-stranded region susceptible to RNP *trans* cleavage (Fig. 2A).

Initially, we designed three single-stranded DNA (ssDNA) molecules with different target region lengths (22, 18 and 14 nt, respectively) and verified the circularization of ssDNA through gel electrophoresis. The results revealed that circularized ssDNA exhibited a slightly higher migration rate compared to linear ssDNA, with a distinct and singular band, confirming the successful circularization of single-molecule ssDNA (Fig. 2B).

The elongation of circularized molecules leads to a more linear topology in the double-stranded target region resulting in varying background levels for Cir-amplifiers of different lengths in Cas12a reactions. Therefore, we investigated the background values caused by the three Cir-amplifiers in the Fluorescence-Cas12a assay. At a concentration of 25 nM, both linear amplifier (amp) and Cir-amplifier (Cir) were introduced into the Fluorescence-Cas12a reaction. After 1-hour reaction at room temperature, all three amplifiers with different lengths of doublestranded target regions could activate the trans-cleavage activity of Cas12a, leading to the cleavage of the FRET reporter and the generation of fluorescence signals, among which no significant differences were observed (Fig. 2C). Theoretically, due to conformational differences, small circular structure (Cir) is expected to be less prone to binding by RNP compared to its corresponding linear structure (amp); consequently, Cir-amplifier reactions would exhibit lower fluorescence values than the linear amplifiers do. Consistent with this hypothesis, the results demonstrate that the fluorescence values produced by Cir-amplifiers activating RNP are approximately 35 to 70 times lower than those produced by corresponding amplifiers (Fig. 2C). This indicates that the circular structure effectively 'locks' the ability of Cir-amplifier to activate RNP. However, as the size of the Cir-amplifier's ring increases, the accessibility of the Cas12a targeted region on its local structure increases, diminishing the effectiveness of this 'lock' and resulting in higher fluorescence values. Under the activation of Cir-amplifier 1 and Cir-amplifier 2, the Cas12a reactions generated fluorescence background values significantly higher than the NC. The fluorescence background value produced by Cir-amplifier 3 with the shortest doublestranded region was only slightly higher than that of the NC (Fig. 2C). Therefore, Cir-amplifier 3 was selected as the enhancer for subsequent assays.

Subsequently, the Cir-amplifier 3 was re-linearized by RNP-0 (Figure S3), and the ability of the re-linearized Cir-amplifier 3 (re-Lin-Cir3) to activate RNP targeting Pg was validated. As shown in Fig. 2D, the experimental group, containing the re-Lin-Cir3 produced by RNP-0 trans cleavage, showed fluorescence values significantly higher than the CTRL group, indicating that the re-Lin-Cir3 possesses the capability to further activate RNP in the subsequent Cas12a reaction.

3.3. Cir-amplifier enhanced Fluorescence-Cas12a assays

The aforementioned results demonstrated that the circular structure effectively 'locks' the activation of Cir-amplifier on RNP. Moreover, upon re-linearization, the Cir-amplifier retains its capability to activate RNP. In the Cas12a reaction with the addition of Cir-amplifier, a small amount of target Pg DNA-activated RNP can cleave both the Ciramplifier and the reporter in the mixture, thereby generating fluorescence signals and a small quantity of re-linearized Cir-amplifier. These re-linearized Cir-amplifiers can subsequently activate a large amount of additional Cas12a RNPs in the mixture, leading to a cascade reaction (Fig. 3A).

However, as preliminary experiments indicated that Cir-amplifier can possess a certain level of leakage to initiate a low level of RNP activation, causing elevated background signal (Fig. 2C), we first explored the concentration of Cir-amplifier in the reaction. We used DNA from 3.9×10^4 CFU of Pg in the reaction, an amount that is undetectable in the standard Fluorescence-Cas12a assays without Ciramplifier (Fig. 1C). After a 1-hour reaction with the addition of Ciramplifier, even at the lowest concentration (25 nM), the experimental group's fluorescence values were significantly higher than that of NC, demonstrating the enhancing effect of Cir-amplifier (Fig. 3B). As the

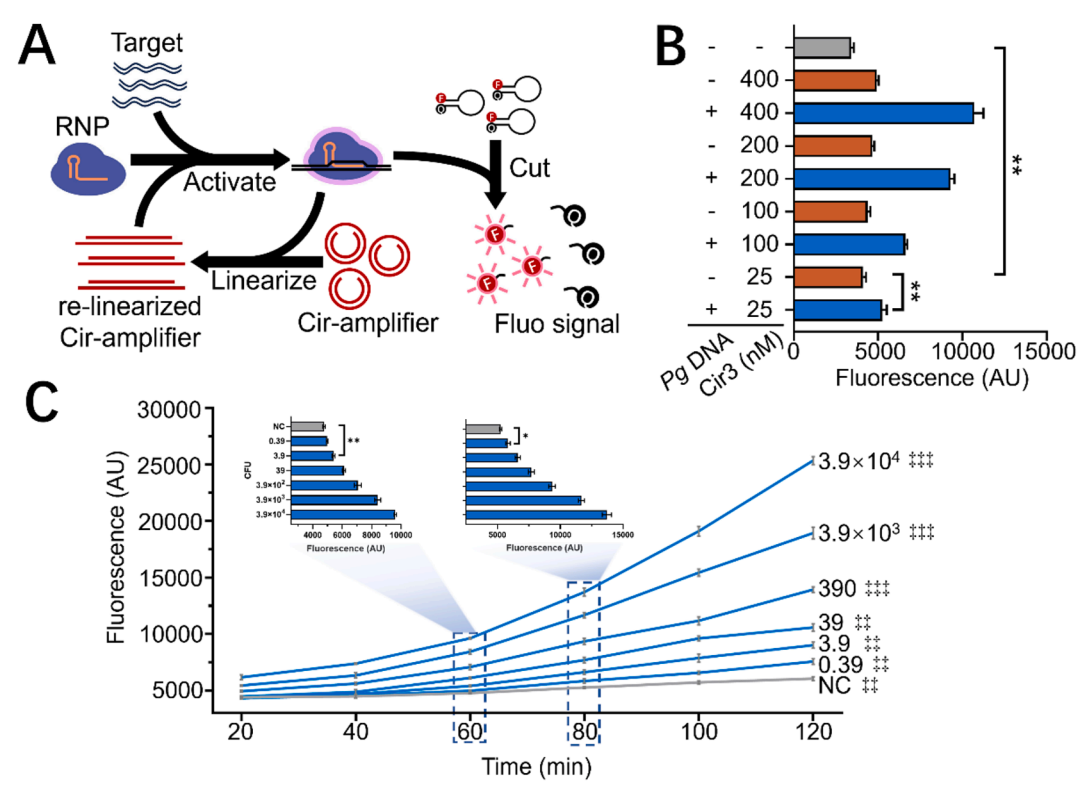


Fig. 3. Cir-amplifier enhanced Fluorescence-Cas12a Assay for the Detection of Pg. (A) Schematic representation of the Cir-amplifier enhanced fluorescence-Cas12a assay. The red solid circle labeled "F" represents the Texas red fluorescence moiety, while "Q" denotes the BHQ-2 quencher moiety. (B) The enhancement effect of different concentrations of Cir-amplifier on the Cas12a reaction. Values represent mean \pm SEM (n = 3, two-tailed Student *t*-test; **, p < 0.01). (C) LoD for the Cir-amplifier enhanced fluorescence-Cas12a assay The X-axis represents reaction time, with corresponding Pg CFU numbers annotated on the right side of the line graph. The fluorescence signal values at the two time points, 60 min and 80 min, are depicted in separate bar graphs. Values represent mean \pm SEM (n = 3, two-tailed Student *t*-test: *, p < 0.05; **, p < 0.01; one-way ANOVA: ‡‡, p < 0.01, ‡‡‡, p < 0.001). (For interpretation of the references to color in this figure legend, the reader is referred to the web version of this article.)

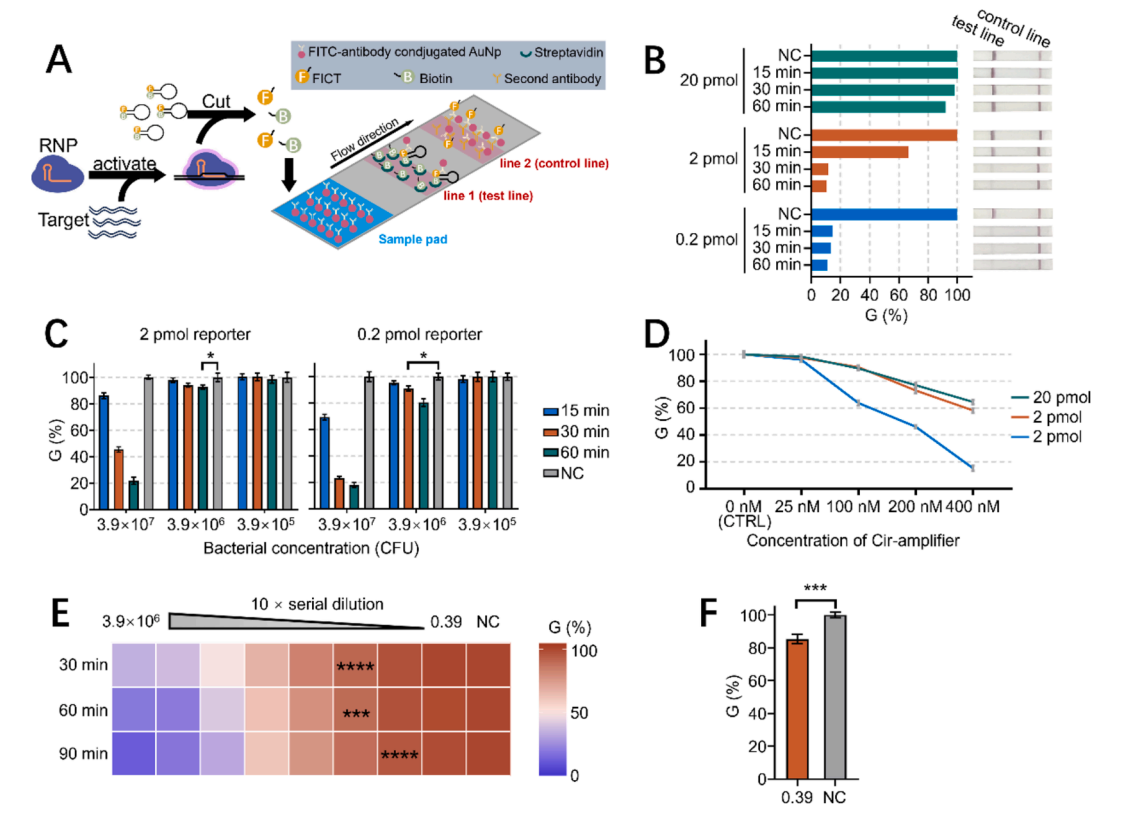


Fig. 4. LFD-Cas12a Assays for the Detection of Pg. (A) Schematic representation of the LFD-Cas12a assay. The yellow solid circle labeled "F" represents the FITC moiety, while "B" denotes the biotin moiety, and the red solid circle represents AuNPs. (B) Cas reactions with different amounts of reporter exhibit variations in the grayscale intensity changes of the test line on the LFD. The histogram represents the G values of the test lines, and the corresponding LFDs were presented on the right. (C) Sensitivity studies for the LFD-Cas12a assays. Values represent mean \pm SEM (n = 3, two-tailed Student t-test; *, p < 0.05; **, p < 0.01). (D) Background caused by Cir-amplifier. The three lines represent reactions containing varying amounts of reporter. Values represent mean \pm SEM (n = 3). (E) Sensitivity of the enhanced LFD-Cas12a assay. The heatmap represents mean G values (n = 3, two-tailed Student t-test; ***, p < 0.001; ****, p < 0.0001). (F) The enhanced LFD-Cas12a detected 0.39 CFU of Pg with a Cas reaction time of 180 min. Values represent mean \pm SEM (n = 3, two-tailed Student t-test; ***, p < 0.001). (For interpretation of the references to color in this figure legend, the reader is referred to the web version of this article.)

quantity of Cir-amplifier increased, the fluorescence values in the experimental group also showed a notable increase. The fluorescence value in the reaction with 400 nM Cir-amplifier was approximately twice that of the 25 nM Cir-amplifier reaction. However, the increase in Cir-amplifier amounts also elevated the background signal of the reaction. Considering the amplification effect and the increase in background signal caused by Cir-amplifier, we selected a concentration of 200 nM Cir-amplifier for subsequent experiments.

We further evaluated the sensitivity of the Cir-amplifier enhanced Fluorescence-Cas12a assay through gradient dilutions of Pg DNA. Under the activation of DNA from 3.9×10^4 CFU, a significant increase in fluorescence values was observed after a 20-minute Cir-amplifier enhanced Cas12a reaction compared with the NC. In contrast to the standard Fluorescence-Cas12a reaction, the enhanced Cas12a reaction achieved a remarkable improvement, detecting as low as 3.9 CFU after 60 min, indicating a 10^5 -fold enhancement of sensitivity (3.9 \times 10^5 vs 3.9 CFU). Furthermore, the fluorescence values of each reaction showed a significant increase over time. Notably, reactions with Pg DNA exhibited a higher rate of fluorescence increase than NC. By 80 min, the fluorescence value of the 0.39 CFU reaction was significantly higher than that of the NC, indicating that the LoD had further decreased to 0.39 CFU, representing a 10⁶-fold enhancement in sensitivity compared to the standard Fluorescence-Cas12a reaction (3.9 \times 10⁵ vs 0.39 CFU) (Fig. 3C). These results indicate that the Cir-amplifier can significantly enhance the detection sensitivity of the Fluorescence-Cas12a assay.

3.4. The LFD-Cas12a assays

LFDs are well-established, portable tools commonly used for the output of results in both nucleic acid and non-nucleic acid substance detection. In LFDs, the target substance modified with FITC and biotin acts as a bridge to capture AuNPs from the sample pad onto line 1 through the binding between biotin and streptavidin. The aggregation of AuNPs turns line 1 red, thus detecting the presence of the target substance.

To facilitate an end-user friendly observable output for the developed Cas12a assays targeting the *Pg* 16S gene, we have integrated the Cas12a reaction with an LFD. The cleavage of the FITC and biotin modified reporter by Cas12a results in a reduction of indirectly bound AuNPs on line 1 (test line), thereby lowering the grayscale value of line 1 (test line) (Fig. 4A).

We initially employed the standard Fluorescence-CRISPR/Cas12a assays components with 20 pmol of FITC and biotin modified reporter per reaction for the LFD-Cas12a detection of the DNA from 3.9×10^8 CFU of Pg. After a 60-minute Cas12a reaction, compared with the NC reaction without target Pg DNA, the test line color did not show a significant change, although the G value slightly decreased (Fig. 4B). We hypothesize that this may be attributed to an excessive reporter amount, where, in the absence of pre-amplification, the amount of reporter cleaved by Cas12a, which is activated by a limited quantity of targeted Pg gene, is relatively low compared to the residual intact reporter in the reaction mixture, resulting in subtle changes in color and grayscale intensity. Subsequently, we reduced the amount of reporter in the Cas12a reaction mixture. When 2 pmol of reporter was used, a slight lightening

of the test line color was observed after a 15-minute Cas12a reaction compared with NC, and the change enlarged when Cas12a reaction lasted for 30 min, with G value dropping below 20 %. Further reduction of the reporter amount to 0.2 pmol resulted in a visible change in the color of the test line compared with the NC reaction with a 15-minute Cas12a reaction, and the G value also dropped below 20 % (Fig. 4B).

We further assessed the sensitivity of the reactions with 2 pmol and 0.2 pmol reporters. The results revealed that with 2 pmol reporter, the Cas12a reaction required 60 min to detect 3.9 \times 10 6 CFU of Pg, while with a 0.2 pmol reporter, the Cas12a reaction achieved detection of 3.9 \times 10 6 CFU of Pg in 30 min. However, neither of these reactions could detect 3.9 \times 10 5 CFU of Pg (Fig. 4C). In terms of specificity, consistent with the standard Fluorescence-Cas12a reactions, LFD-Cas12a exhibited reactivity exclusively towards Pg DNA (Figure S4).

Subsequently, the Cir-amplifier was introduced to improve the sensitivity of the LFD-Cas12a assay. In the Fluorescence-Cas12a reactions, the Cir-amplifier was observed to leak in activating the RNP, albeit to a low extent; more importantly, the Cir-amplifier carries a biotin modification on its nanostructure, potentially leading to competition with the biotin-modified reporter in the LFD-Cas12a reaction for binding to the streptavidin on the test line of the LFD, which has not been investigated in the previous study [23]. Both factors can potentially contribute to a reduction in the grayscale of the test line, thus increasing the background. Therefore, we investigated the background values caused by the introduction of Cir-amplifier with varying amounts of reporter in LFD-Cas12a reactions. As shown in Fig. 4D, compared with the control reaction (CTRL) with 0 nM Cir-amplifier, when the Cas12a reaction included only 0.2 pmol of the reporter, 100 nM Cir-amplifier led to a decrease in G value to around 60 %, while 400 nM Ciramplifier resulted in a reduction to below 20 %. For LFD-Cas12a reactions containing 20 pmol and 2 pmol reporters, although the background values increased with the addition of more Cir-amplifier, even with the inclusion of 200 nM Cir-amplifier, the G value remained above 70 %. Considering that 20 pmol of reporter is an excessive amount for the LFD-Cas12a reaction (Fig. 4B), subsequent experiments adopted the combination of 2 pmol reporter and 200 nM Cir-amplifier.

After determining the optimal quantities of the reporter and Cir-

amplifier, we evaluated the LoD of the Cir-amplifier enhanced LFD-Cas12a assay. The results showed that as the Cas12a reaction time increased, the LoD decreased (Fig. 4E). When the Cas12a reaction lasted for 30 min and 60 min, the assay displayed a significant decrease in G value of the test line below the NC at the activation of 39 CFU Pg DNA. With the Cas12a reaction time extended to 90 min, the LoD decreased to 3.9 CFU (Fig. 4E). To investigate whether the Cir-amplifier enhanced LFD-Cas12a assay could achieve sensitivity comparable to the enhanced Fluorescence-Cas assay, we prolonged the Cas12a reaction time for the 0.39 CFU of Pg DNA to 180 min. The results showed a significant decrease in the G value of the test line below the NC on the LFD (Fig. 4F), indicating that, with sufficient Cas12a reaction time, the Cir-amplifier enhanced LFD-Cas12a could also achieve a sensitivity comparable to the Cir-amplifier enhanced Fluorescence-Cas12a reaction, but in an enduser friendly manner without the need for any instrument and without amplicon generation to the testing environment.

3.5. Clinical sample study

To evaluate the performance of the developed Cir-amplifier enhanced assays in detecting real clinical samples, we established an RT-PCR method targeting the same region as a reference. Among the 131 plaque clinical samples tested, 80 showed RT-PCR-positive results, and all of which were also positive in both Cir-amplifier enhanced Fluorescence- and LFD-Cas12a assays (Fig. 5). Among the 51 RT-PCR-negative samples, 5 were positive in both Cir-amplifier enhanced Fluorescence- and LFD-Cas12a assays, and 1 was positive only in the Cir-amplifier enhanced Fluorescence-Cas12a assay (Fig. 5). Given the variations in Pg content across samples, the observed differences in positive results among samples are likely attributed to the varying sensitivities of the detection assays. All 45 samples concurrently identified as negative by Cir-amplifier enhanced Fluorescence- and LFD-Cas12a assays were found to be RT-PCR-negative as well, indicating both Cas12a assays possess 100 % sensitivity with the RT-PCR method.

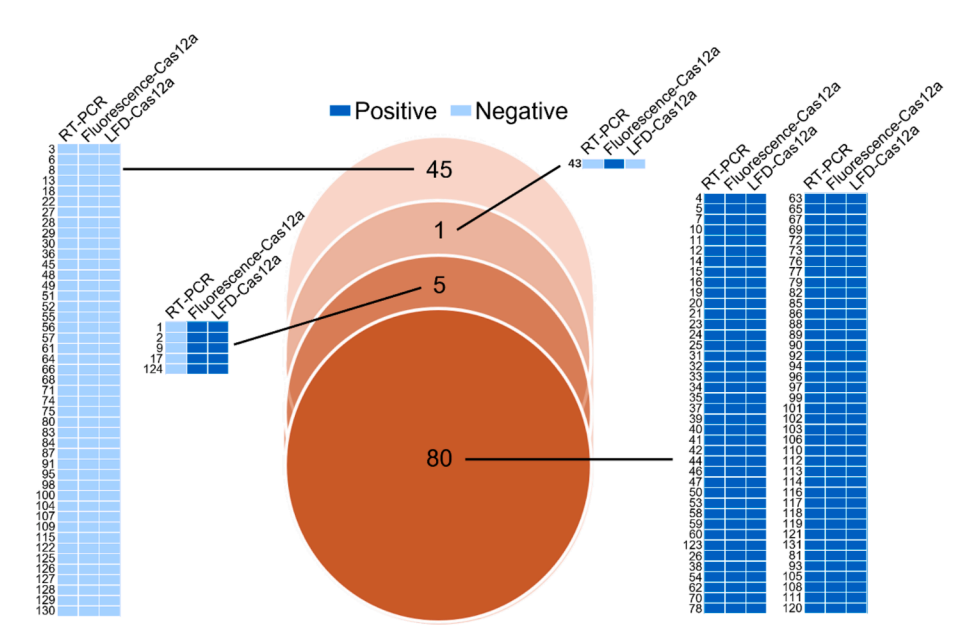


Fig. 5. Detection of *Pg* **in subgingival plaque samples by RT-PCR and Cas12a assays.** The four shades of orange, from dark to light, respectively represent: all three methods showing positive results, two Cir-amplifier enhanced Cas12a assays showing positive results but RT-PCR showing negative results, only the Ciramplifier enhanced fluorescence-Cas12a assay showing positive results, and all three assays showing negative results. The specific positive/negative results are displayed in a binary plot next to the Venn diagram, with the numbers on the left side of the binary plot representing the sample IDs. Dark blue indicates positive results, while light blue indicates negative results. (For interpretation of the references to color in this figure legend, the reader is referred to the web version of this article.)

4. Discussion

To maximize the sensitivity of the assays, we incorporated a hairpin reporter into the reaction, which has been previously demonstrated to be more efficiently cleaved by Cas enzymes compared to an ssDNA reporter [24,25]. Despite the improvement in sensitivity achieved by utilizing the hairpin reporter with ssDNA, the LoD of 3.9×10^5 CFU is still insufficient for clinical applications [13]. Therefore, additional strategies to enhance sensitivity are desired. Generally, an increased quantity of targets has the capacity to activate a greater number of RNPs, thereby eliciting heightened trans-endonuclease activity and subsequently yielding a more robust signal. This phenomenon underscores the necessity for target pre-amplification to augment detection sensitivity in CRISPR/Cas biosensors, as previously documented in systems such as SHERLOCK et al. [20]. However, to mitigate the aforementioned adverse effects associated with pre-amplification, we have devised a strategy that augments the quantity of targets within the Cas12a reaction system without the necessity for pre-amplification.

Considering the strict dependence of interactions among biomacromolecules on their structures, we hypothesize that target DNA with intricate topological configurations, such as circular structures, may not undergo smooth binding by RNPs and subsequent activation of their *trans* activity, unlike linear targets. Consistent with our previous investigations, the findings of this study indicate a notable disparity in the activation of Cas12a enzyme *trans* activity between linear and circular targets (Cir-amplifier) [23]. By synthesizing a Cir-amplifier targeting the Pg specific gene, results demonstrate that the incorporation of the Cir-amplifier significantly enhances the efficiency of signal generation in the Cas12a reaction, elevating the sensitivity of Pg detection by a factor of 10^6 .

The Cir-amplifier enhanced Fluorescence-Cas12a assay established here exhibits satisfactory sensitivity. However, fluorescence signal readout still requires fluorescent readout instruments. In order to establish a naked-eye detectable method with uncompromised sensitivity, we combined the Cir-amplifier enhanced Cas12a reaction with LFD to offer advantages such as low cost, a simple fabrication process, and independence from external instruments. In prior proceed the LFD-Cas12a signal reading methods, a significant amount of reporter molecules was often required to block all AuNPs onto line 1 [23,27,28]. This setup allowed line 2 to exhibit a red color only in positive reactions when the reporter was cleaved (Fig. 4A). Initially attempting this approach, even with an increased reporter quantity of 30 pmol per reaction in negative Cas12a reactions, we could not completely prevent the coloration of line 2 (Figure S5). Further increasing the reporter quantity would result in prohibitive detection costs. Therefore, we designated line 1 as the test line and, by observing changes in color and grayscale after Cas12a reaction, determined the detection results. The results demonstrate that this method requires only 0.2 pmol of reporter per reaction, saving at least 100 times the amount of reporter used previously [23,27,28]. The introduction of the Cir-amplifier also significantly enhances the sensitivity of the LFD-Cas assay by a factor of 10^{6} .

Achieving ultra-high sensitivity in nucleic acid detection without pre-amplification is a major challenge for CRISPR/Cas biosensing in real-life point-of-care test (POCT) applications. Previously reported pre-amplification-free CRISPR/Cas systems have mainly focused on improving signal output to enhance detection sensitivity [29–31]. The signal enhancement strategy in this study demonstrated that the Ciramplifier is a simple, robust and versatile approach to overcome this challenge. Unlike previously reported pre-amplification Cas assays [22,27,32], the signal-enhancing effect of the Ciramplifier in this study increases over time. This is because, initially, there is a low amount of linearized target in the mixture. As more Ciramplifiers re-linearized, the reaction signal gradually intensifies. The two Ciramplifier enhanced assays can achieve high-sensitivity target detection within a time frame similar to traditional PCR reactions, about 60 to 90 min, with LoDs of

0.39 CFU for the Fluorescence-Cas12a reaction and 3.9 CFU for the LFD-Cas12a reaction (Fig. 3C and 4E). However, as a POCT, faster detection is preferable. Future work should focus on shortening the reaction time. The Cir-amplifier is key to achieving pre-amplification-free reactions, and further optimization of the Cir-amplifier sequence is one of the important strategies. Optimizing the sequence and length of the singlestranded region of the Cir-amplifier could make it easier for RNP transcleavage, leading to faster linearization. Simultaneously, adjusting the overall size of the Cir-amplifier, while ensuring improved blockage effect of circle structure to RNP activation and highly efficient RNP recognition after linearization, can reduce background noise, allowing more Cir-amplifier to be used in the reaction. Additionally, the amount and activity of Cas12a enzyme directly affect the reaction speed. Increasing the amount of Cas12a within a reasonable cost range or finding Cas orthologues with higher cleavage efficiency could also shorten the reaction time. Since the introduction of the Cir-amplifier in this study did not significantly alter the well-known standard Cas12a reaction systems, it can be directly and easily integrated with other existing Cas reaction enhancement strategies, such as using multiple gRNAs to enhance RNP target recognition [31].

Culture isolation has long been considered the gold standard for Pg detection. However, it's time-consuming, labor-intensive, and their outcomes can be influenced by factors such as the interval between sampling and cultivation, the transport medium used, and the selection of culture media and conditions [12]. Several non-culturing diagnostic methods have been reported and commercially applied in clinical settings, including DNA probe techniques, enzyme-linked immunosorbent assay (ELISA), and bacterial marker detecting methods [33,34]. These methods have not been widely adopted in clinical diagnostics due to inherent flaws, including insufficient sensitivity, complex procedures, or the inability to identify specific pathogen species [33]. Nucleic acid detection techniques offer a faster and more sensitive alternative. Several PCR methods have been reported to efficiently and sensitively detect Pg with high specificity [8,11,12]. However, the reliance on thermal cycling equipment limits the versatility of PCR in various settings. Although the application of isothermal amplification techniques reduces the need for specialized equipment [13], nucleic acid amplification methods pose the risk of aerosol contamination due to the amplification of large numbers of target sequences, potentially leading to false-positive results in subsequent experiments. Compared to these developed methods, the two pre-amplification-free Cir-amplifier enhanced Cas12a reactions in this study offer high sensitivity while eliminating the risk of contamination associated with nucleic acid amplification. Additionally, they can operate at room temperature and have low equipment requirements. The Fluorescence-Cas12a reaction only requires standard fluorescence signal reading equipment, while the LFD-Cas12a reaction can be observed with the naked eye or analyzed for test line grayscale using a personal computer. Microfluidics-based CRISPR/Cas systems, by isolating reactions within discrete microdroplets, allow for highly precise detection, down to single-molecule or single-cell levels, making them particularly valuable for high-resolution applications. Additionally, they are compatible with advanced sorting technologies, such as fluorescence-activated cell sorting (FACS), enabling high-throughput screening [35,36]. However, the need for specialized microfluidic equipment can limit their use in resourceconstrained environments. In contrast, the simplicity of operation and low equipment dependency are advantages of Cir-amplifier-enhanced Cas12a reactions, which are crucial for clinical testing. Furthermore, the removal of the pre-amplification step, which is required in most CRISPR/Cas systems [37], simplifies the procedure, saving time, reducing human error, and easing the workload on healthcare personnel. Extracted DNA only needs to be added to the Cas12a reaction premix, without the need for complex reagent preparation and liquid transfer steps. These features make Cir-amplifier enhanced Cas12a reactions highly versatile, even in resource-limited regions, making them an ideal option for chair-side or end-user Pg detection. Considering the

complexity of actual clinical samples, 131 plaque clinical samples were used to test the Cir-amplifier enhanced Cas12a reactions and were compared in parallel with the RT-PCR method. The results showed that all samples detected as positive by RT-PCR were also detected as positive by the Cas12a reactions, further proving its value for real-life pathogen diagnosis.

5. Conclusion

This study presents, for the first time, the utilization of the CRISPR/ Cas system for Pg DNA detection, with findings conveyed through fluorescence signals or LFD presentation in an amplification-free manner. Facilitated by the specially designed Cir-amplifier to induce the CRISPR/Cas cascade reaction, the enhanced Pg detection sensitivity of a standard Fluorescence-Cas12a reaction can easily reach 0.39 CFU per reaction, while the LFD-Cas reaction achieves a sensitivity of 3.9 CFU per reaction under the same experimental setup as any other standard CRISPR/Cas12a reactions. The Pg detection techniques associated with CRISPR/Cas12a, as developed in this investigation, offer a highly sensitive and adaptable approach for cost-effective Pg diagnostics. Moreover, the results indicate that the Cir-amplifier, serving as a CRISPR/Cas reaction enhancer, can be applied to CRISPR/Cas systems producing various signal formats. This introduces a pioneering method for the rapid, point-of-care, and highly sensitive measurement of nucleic acids without the need for intensively trained expert.

Fundings

This work was supported by the National Natural Science Foundation of China [grant numbers 32060024, 32000088] and the Natural Science Foundation of Hunan Province [grant number 2022JJ40050].

CRediT authorship contribution statement

Xuan Wu: Writing – original draft, Visualization, Methodology, Investigation, Funding acquisition, Conceptualization. Ning-Ning Pi: Methodology, Investigation. Fei Deng: Methodology, Investigation. Shi-Yang Tang: Methodology, Data curation. Cheng-Chen Zhang: Investigation, Data curation. Lu Zhu: Investigation. Fang-Fang Sun: Visualization. Xiao-Yao He: Conceptualization. Han-Qing Li: Methodology. Shi-Long Zhao: Methodology. Rong Xiang: Writing – original draft, Methodology, Investigation, Funding acquisition. Yi Li: Writing – review & editing, Writing – original draft, Supervision, Methodology, Conceptualization.

Declaration of competing interest

The authors declare that they have no known competing financial interests or personal relationships that could have appeared to influence the work reported in this paper.

Appendix A. Supplementary data

Supplementary data to this article can be found online at https://doi.org/10.1016/j.microc.2024.111983.

Data availability

Data will be made available on request.

References

- [1] N.J. Kassebaum, E. Bernabé, M. Dahiya, B. Bhandari, C.J.L. Murray, W. Marcenes, Global Burden of Severe Periodontitis in 1990–2010, J. Dent. Res. 93 (2014) 1045–1053.
- [2] P.I. Eke, B.A. Dye, L. Wei, G.D. Slade, G.O. Thornton-Evans, W.S. Borgnakke, G.W. Taylor, R.C. Page, J.D. Beck, R.J. Genco, Update on Prevalence of Periodontitis in

- Adults in the United States: NHANES 2009 to 2012, J. Periodontol., 86 (2015) 611-
- [3] A. Hugoson, B. Sjödin, O. Norderyd, Trends over 30 years, 1973–2003, in the prevalence and severity of periodontal disease, J. Clin. Periodontol. 35 (2008) 405–414.
- [4] P. Bullon, H.N. Newman, M. Battino, Obesity, diabetes mellitus, atherosclerosis and chronic periodontitis: a shared pathology via oxidative stress and mitochondrial dysfunction? Periodontology 2000 (64) (2014) 139–153.
- [5] S. Yang, L.S. Zhao, C. Cai, Q. Shi, N. Wen, J. Xu, Association between periodontitis and peripheral artery disease: a systematic review and meta-analysis, BMC Cardiovasc. Disord. 18 (2018).
- [6] A.R. Kamer, E. Pirraglia, W. Tsui, H. Rusinek, S. Vallabhajosula, L. Mosconi, L. Yi, P. McHugh, R.G. Craig, S. Svetcov, R. Linker, C. Shi, L. Glodzik, S. Williams, P. Corby, D. Saxena, M.J. de Leon, Periodontal disease associates with higher brain amyloid load in normal elderly, Neurobiol. Aging 36 (2015) 627–633.
- [7] H.-C. Chan, C.-T. Wu, K.B. Welch, W.J. Loesche, Periodontal Disease Activity Measured by the Benzoyl-DL-Arginine-Naphthylamide Test Is Associated With Preterm Births, J. Periodontol. 81 (2010) 982–991.
- [8] C. Gaertig, K. Niemann, J. Berthold, L. Giel, N. Leitschuh, C. Boehm, L. Roussak, K. Vetter, D. Kuhlmeier, Development of a point-of-care-device for fast detection of periodontal pathogens, BMC Oral Health 15 (2015).
- [9] W. He, M. You, W. Wan, F. Xu, F. Li, A. Li, Point-of-Care Periodontitis Testing: Biomarkers, Current Technologies, and Perspectives, Trends Biotechnol. 36 (2018) 1127–1144.
- [10] N. Bostanci, G.N. Belibasakis, Porphyromonas gingivalis: an invasive and evasive opportunistic oral pathogen, FEMS Microbiology Letters, Microbiol Letters 333 (2012) 1–9.
- [11] S. Eick, A. Straube, A. Guentsch, W. Pfister, H. Jentsch, Comparison of real-time polymerase chain reaction and DNA-strip technology in microbiological evaluation of periodontitis treatment, Diagn. Microbiol. Infect. Dis. 69 (2011) 12–20.
- [12] K. Boutaga, A.J. van Winkelhoff, C.M.J.E. Vandenbroucke-Grauls, P.H. M. Savelkoul, Comparison of Real-Time PCR and Culture for Detection of Porphyromonas gingivalis in Subgingival Plaque Samples, J. Clin. Microbiol. 41 (2003) 4950–4954.
- [13] D. Ge, F. Wang, Y. Hu, B. Wang, X. Gao, Z. Chen, Fast, Simple, and Highly Specific Molecular Detection of Porphyromonas gingivalis Using Isothermal Amplification and Lateral Flow Strip Methods, Front Cell Infect Microbiol 12 (2022) 895261.
- [14] D. Davidi, S. Fitzgerald, H.L. Glaspell, S. Jalbert, C.M. Klapperich, L. Landaverde, S. Maheras, S.E. Mattoon, V.M. Britto, G.T. Nguyen, Amplicon residues in research laboratories masquerade as COVID-19 in surveillance tests, Cell Reports Methods 1 (2021).
- [15] O.O. Abudayyeh, J.S. Gootenberg, S. Konermann, J. Joung, I.M. Slaymaker, D. B. Cox, S. Shmakov, K.S. Makarova, E. Semenova, L. Minakhin, K. Severinov, A. Regev, E.S. Lander, E.V. Koonin, F. Zhang, C2c2 is a single-component programmable RNA-guided RNA-targeting CRISPR effector, Science 353 (2016) aaf5573.
- [16] S.Y. Li, Q.X. Cheng, J.K. Liu, X.Q. Nie, G.P. Zhao, J. Wang, CRISPR-Cas12a has both cis- and trans-cleavage activities on single-stranded DNA, Cell Res 28 (2018) 491–493.
- [17] J.S. Chen, E. Ma, L.B. Harrington, M. Da Costa, X. Tian, J.M. Palefsky, J.A. Doudna, CRISPR-Cas12a target binding unleashes indiscriminate single-stranded DNase activity, Science 360 (2018) 436–439.
- [18] J.S. Gootenberg, O.O. Abudayyeh, J.W. Lee, P. Essletzbichler, A.J. Dy, J. Joung, V. Verdine, N. Donghia, N.M. Daringer, C.A. Freije, C. Myhrvold, R. P. Bhattacharyya, J. Livny, A. Regev, E.V. Koonin, D.T. Hung, P.C. Sabeti, J. J. Collins, F. Zhang, Nucleic acid detection with CRISPR-Cas13a/C2c2, Science 356 (2017) 438–442.
- [19] L.B. Harrington, D. Burstein, J.S. Chen, D. Paez-Espino, E. Ma, I.P. Witte, J. C. Cofsky, N.C. Kyrpides, J.F. Banfield, J.A. Doudna, Programmed DNA destruction by miniature CRISPR-Cas14 enzymes, Science 362 (2018) 839–842.
- [20] C. Myhrvold, C.A. Freije, J.S. Gootenberg, O.O. Abudayyeh, H.C. Metsky, A. F. Durbin, M.J. Kellner, A.L. Tan, L.M. Paul, L.A. Parham, K.F. Garcia, K.G. Barnes, B. Chak, A. Mondini, M.L. Nogueira, S. Isern, S.F. Michael, I. Lorenzana, N. L. Yozwiak, B.L. MacInnis, I. Bosch, L. Gehrke, F. Zhang, P.C. Sabeti, Field-deployable viral diagnostics using CRISPR-Cas13, Science 360 (2018) 444–448.
- [21] J.P. Broughton, X. Deng, G. Yu, C.L. Fasching, C.Y. Chiu, CRISPR–Cas12-based detection of SARS-CoV-2, Nat. Biotechnol. 38 (2020) 870–874.
- [22] F. Li, Q. Ye, M. Chen, X. Xiang, J. Zhang, R. Pang, L. Xue, J. Wang, Q. Gu, T. Lei, X. Wei, Y. Ding, Q. Wu, Cas12aFDet: A CRISPR/Cas12a-based fluorescence platform for sensitive and specific detection of Listeria monocytogenes serotype 4c, Anal Chim Acta 1151 (2021) 338248.
- [23] F. Deng, Y. Li, B. Yang, R. Sang, W. Deng, M. Kansara, F. Lin, S. Thavaneswaran, D. M. Thomas, E.M. Goldys, Topological barrier to Cas12a activation by circular DNA nanostructures facilitates autocatalysis and transforms DNA/RNA sensing, Nat. Commun. 15 (2024).
- [24] M. Rossetti, R. Merlo, N. Bagheri, D. Moscone, A. Valenti, A. Saha, P.R. Arantes, R. Ippodrino, F. Ricci, I. Treglia, E. Delibato, J. van der Oost, G. Palermo, G. Perugino, A. Porchetta, Enhancement of CRISPR/Cas12a trans-cleavage activity using hairpin DNA reporters, Nucleic Acids Res. 50 (2022) 8377–8391.
- [25] T. Luo, J. Li, Y. He, H. Liu, Z. Deng, X. Long, Q. Wan, J. Ding, Z. Gong, Y. Yang, S. Zhong, Designing a CRISPR/Cas12a- and Au-Nanobeacon-Based Diagnostic Biosensor Enabling Direct, Rapid, and Sensitive miRNA Detection, Anal. Chem. 94 (2022) 6566–6573.
- [26] C.A. Schneider, W.S. Rasband, K.W. Eliceiri, NIH Image to ImageJ: 25 years of image analysis, Nat Methods 9 (2012) 671–675.

- [27] J.P. Broughton, X. Deng, G. Yu, C.L. Fasching, V. Servellita, J. Singh, X. Miao, J. A. Streithorst, A. Granados, A. Sotomayor-Gonzalez, K. Zorn, A. Gopez, E. Hsu, W. Gu, S. Miller, C.Y. Pan, H. Guevara, D.A. Wadford, J.S. Chen, C.Y. Chiu, CRISPR-Cas12-based detection of SARS-CoV-2, Nat Biotechnol 38 (2020) 870–874.
- [28] G. Su, M. Zhu, D. Li, M. Xu, Y. Zhu, Y. Zhang, H. Zhu, F. Li, Y. Yu, Multiplexed lateral flow assay integrated with orthogonal CRISPR-Cas system for SARS-CoV-2 detection, Sens Actuators B Chem 371 (2022) 132537.
- [29] A. Santiago-Frangos, L.N. Hall, A. Nemudraia, A. Nemudryi, P. Krishna, T. Wiegand, R.A. Wilkinson, D.T. Snyder, J.F. Hedges, C. Cicha, H.H. Lee, A. Graham, M.A. Jutila, M.P. Taylor, B. Wiedenheft, Intrinsic signal amplification by type III CRISPR-Cas systems provides a sequence-specific SARS-CoV-2 diagnostic, Cell Reports Medicine 2 (2021).
- [30] D. Samanta, S.B. Ebrahimi, N. Ramani, C.A. Mirkin, Enhancing CRISPR-Cas-Mediated Detection of Nucleic Acid and Non-nucleic Acid Targets Using Enzyme-Labeled Reporters, J Am Chem Soc 144 (2022) 16310–16315.
- [31] P. Fozouni, S. Son, M. Díaz de León Derby, G.J. Knott, C.N. Gray, M.V. D'Ambrosio, C. Zhao, N.A. Switz, G.R. Kumar, S.I. Stephens, D. Boehm, C.-L. Tsou, J. Shu, A. Bhuiya, M. Armstrong, A.R. Harris, P.-Y. Chen, J.M. Osterloh, A. Meyer-Franke, B. Joehnk, K. Walcott, A. Sil, C. Langelier, K.S. Pollard, E.D. Crawford, A.S. Puschnik,

- M. Phelps, A. Kistler, J.L. DeRisi, J.A. Doudna, D.A. Fletcher, M. Ott, Amplification-free detection of SARS-CoV-2 with CRISPR-Cas13a and mobile phone microscopy, Cell, 184 (2021) 323-333.e329.
- [32] F. Hu, Y. Liu, S. Zhao, Z. Zhang, X. Li, N. Peng, Z. Jiang, A one-pot CRISPR/Cas13a-based contamination-free biosensor for low-cost and rapid nucleic acid diagnostics, Biosens Bioelectron 202 (2022) 113994.
- [33] N. Srivastava, P.A. Nayak, S. Rana, Point of Care- A Novel Approach to Periodontal Diagnosis-A Review, J Clin Diagn Res 11 (2017) ZE01-ZE06.
- [34] N.M. O'Brien-Simpson, K. Burgess, G.C. Brammar, I.B. Darby, E.C. Reynolds, Development and evaluation of a saliva-based chair-side diagnostic for the detection of Porphyromonas gingivalis, J Oral Microbiol 7 (2015) 29129.
- [35] Y. Shang, G. Xing, J. Lin, Y. Li, Y. Lin, S. Chen, J.-M. Lin, Multiplex bacteria detection using one-pot CRISPR/Cas13a-based droplet microfluidics, Biosens. Bioelectron. 243 (2024).
- [36] Y. Zhang, H. Liu, Y. Nakagawa, Y. Nagasaka, T. Ding, S.-Y. Tang, Y. Yalikun, K. Goda, M. Li, Enhanced CRISPR/Cas12a-based quantitative detection of nucleic acids using double emulsion droplets, Biosens. Bioelectron. 257 (2024).
- [37] M. Wang, R. Zhang, J. Li, CRISPR/cas systems redefine nucleic acid detection: Principles and methods, Biosens. Bioelectron. 165 (2020).